



Study of pH Dependent Pt Electrodeposition for Hydrogen Production in PV Assisted Water Electrolysis System

Jyotiprakash B. Yadav, Sang-Youn Chae, and Oh-Shim Joo^z

Clean Energy Research Center, Korea Institute of Science and Technology (KIST), Seongbuk-gu, Seoul 130-650, Korea.

The electrodeposition of Pt film is carried out in an electrolytic bath of different pH (pH varied from 2 to 4) at constant potential -0.35V for 30 min. The prepared Pt film is studied by different analyzing techniques as well as used as a cathode electrode in photovoltaic (PV) cell assisted water electrolysis system for hydrogen production. The film properties show strong dependence on pH of electrolytic solution. Pure Pt film with low mass loading ($2.44 \times 10^{-5} \text{ g cm}^{-2}$) is obtained at pH 2, which subsequently undergo oxidation and mass loading also increases with pH. The earth worm like surface morphology is observed in a film deposited at pH 2, which is changed into thorny ball like morphology with pH. The active surface area and the activity for hydrogen evolution show linear relation and decreases with pH. Thus, the highly active Pt film for hydrogen production is obtained at pH 2, which shows about 25% higher hydrogen production and 3500 times lower Pt loading (from 0.07 g cm^{-2} to $2.44 \times 10^{-5} \text{ g cm}^{-2}$) than those of commercial Pt mesh.

© 2011 The Electrochemical Society. [DOI: 10.1149/1.3582766] All rights reserved.

Manuscript submitted December 7, 2010; revised manuscript received March 1, 2011. Published May 3, 2011.

Rising energy demand, dwindling conventional energy sources and global warming, are the major challenges facing the energy future, which are forcing mankind to search for alternative energy sources. Among all alternatives, hydrogen is an attractive one because of its advantageous features such as; high flammability, richest in energy per mass unit, light weight, environmental compatible and direct conversion into thermal, mechanical and electrical energy.¹⁻³ Several production methods including steam reforming, bioconversion and water electrolysis have been studied with impressive results.⁴⁻⁶ Among them, 96% of hydrogen is produced by reforming from fossil fuels and remaining from water electrolysis. Nowadays, water electrolysis is attracting more scientific attention because of its simple, non-polluting and high purity hydrogen production features. Technologically, basics for hydrogen production via water electrolysis have long been known. However, there are some disadvantages such as electricity cost, which is two third of its operation cost.⁷ Hence the electrolysis particularly powered by renewable energy has got a great attention.

In present work, we have used a PV assisted water electrolysis system for hydrogen production, which simply consists of an electrolytic cell and silicon solar cell. In schematic of PV assisted water electrolysis system, silicon solar cell is placed outside the electrolytic cell, which provides biasing current to cathode-anode electrode assembly (in electrolytic cell) for water splitting.⁸ In the cell, the hydrogen evolution efficiency greatly depends on the overpotential for cathodic and anodic reactions, and on internal resistance of electrolytic cell.⁹ These factors depend on catalytic activity of electrode material and its electrochemical stability.

A principal focus of the present work is to design cathode electrode with desirable electrochemical stability and improved electrocatalytic activity towards water splitting reaction. According to Stojic et al.,¹⁰ the electrocatalytic activity of various metals for hydrogen evolution is a function of outer shell electronic configuration. It means catalytic activity increases with d-electrons and reaches to maximum at nearly filled d-orbital. Among all literature known d-orbital transition metals, platinum ($5d^9$ electronic configuration) has an aggressive electro-catalytic activity, biocompatibility and electrochemical stability, which makes it a promising cathode electrode material for water splitting reaction.¹¹⁻¹⁴ Only the cost of Pt is a serious problem. Hence during past few decades, research interest is focused on cost reduction by depositing highly active Pt film on a low cost metal substrate with minimum Pt loading or introducing economic film preparation method.

In previous report, we studied low Pt loading electrospray deposition technique for hydrogen evolution electrode.¹⁵ The hydrogen

evolution performance for this film was 533 ml h^{-1} , wherein, material loading was reduced by 1000 times and performance improved by 26% higher than the commercial Pt mesh (418 ml h^{-1}). However, this technique needed post heat treatment that possibly increases the cost of film preparation. Hence, our intention is to search for a technique, which has no need to do post treatment and can possibly deposit Pt film with minimum loading and high catalytic activity for hydrogen evolution.

Among the several Pt film deposition techniques, electrodeposition has the advantages of being economic, high control over film growth and complex surface deposition ability.¹⁶ Herein, the electrical parameters are main controller of film thickness, morphology and composition. Type of precursor, composition, temperature and pH of electrolytic bath are also play a vital role in electrochemical deposition. There are several reports on Pt film deposited at different precursor solution, composition and temperature.^{16,17} Only few reports are available on pH dependent study of Pt film preparation.¹⁸

Thus by keeping in mind all these aspects, an attempt has been made for Pt films electrodeposition at different pH and characterize those films by different analytical techniques.

Experimental

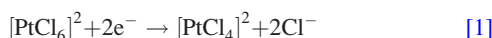
Pt films were electrodeposited on a nickel (Ni) substrate ($9 \times 9 \text{ cm}$) through potentiostat (IviumStat technology, Netherland) by using chrono-amperometric method. The electrolytic bath was prepared by adding $0.5 \text{ mM H}_2\text{PtCl}_6 \cdot 5.7 (\text{H}_2\text{O})$ in distilled water along with continuous stirring, which resulted in yellow transparent solution of pH 3. The pH (2-4) of electrolytic bath was adjusted by using H_2SO_4 and NaOH solution. The electrolytic solution was deoxygenated by bubbling N_2 gas prior to use. The film deposition was carried out on Ni plate for 30 min, in a single cell three electrodes system at a constant potential (-0.35V) and at room temperature, wherein Pt plate and Ag/AgCl (saturated NaCl) were used as counter electrode and reference electrode, respectively. Finally, as prepared Pt film was rinsed with distilled water and dried under the flow of argon gas. The resulted films were characterized by different analyzing techniques such as scanning electron microscopy (SEM-HITACHI S-4100 model) and X-ray photoelectron spectroscopy techniques (XPS-ESCA, PHI-5800 model). The XPS analysis was carried out at excitation energy of 1486.6 eV and a scan step of 0.1 eV . Auger electron spectroscopy (AES-ULVAC-PHI-700) was used for depth profile measurement at beam voltage 5 kV and sputtering rate 150 \AA min^{-1} . The PV assisted water electrolysis system was used for hydrogen evolution study, wherein the silicon solar cell was used for powering the electrochemical cell. The Pt film on Ni substrate was used as a cathode (hydrogen electrode) and stainless

^z E-mail: jooat@kist.re.kr

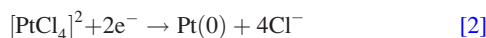
steel (SS) plate as an anode in the electrolytic bath containing 1 M NaOH solution. The silicon solar cell was irradiated by Xenon lamp, whose intensity was fixed at one sun condition by using a reference solar cell (PVM-153). The electrochemical products such as oxygen and hydrogen were measured using a wet-test meter for 5 h with 1 h time lapse.

Results and Discussion

Theoretical growth mechanism.—The common method of Pt electrodeposition involves an electrochemical bath containing Pt(IV) complexes (complexed with chloride, ammine, sulfide, nitride and hydroxyl group). Most of the researchers prefer economic Pt(IV) chloride complex for Pt film deposition, which is followed by a chemical Reaction 1 (Ref. 19)



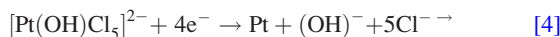
Initially, $[\text{PtCl}_6]^{2-}$ ion reduces to $[\text{PtCl}_4]^{2-}$ by gaining two electrons from the cathode, which further reduces to Pt(0) metal by Reaction 2



The magnitude of Pt film deposition depends on reduction rate of both $[\text{PtCl}_4]^{2-}$ and $[\text{PtCl}_6]^{2-}$ ions. However, in strongly acidic solution, the high concentration of Cl^- ion inhibits the electro-reduction rate of $[\text{PtCl}_4]^{2-}$ ion as compared to $[\text{PtCl}_6]^{2-}$ ion.¹⁹ Equation (1) and (2) are the two steps of single reaction, leading to the formation of Cl^- ions that significantly reduces the rate of Pt deposition. In case of weakly acidic solution ($\text{pH} > 2$), Cl^- ions in the coordination sphere are replaced by OH^- ions and it forms intermediate ions of $[\text{Pt}(\text{OH})_m\text{Cl}_{6-m}]^{2-}$, which contribute to the electrodeposition of Pt film.²⁰



In equation (3), the value of 'm' increases (from 0 to 6) with concentration of OH^- ions or pH of electrolytic bath. Thus, the pH of electrolytic bath play a crucial role in the formation of $[\text{PtCl}_6]^{2-}$ and intermediate ions of $[\text{Pt}(\text{OH})_m\text{Cl}_{6-m}]^{2-}$ that strongly affect the growth mechanism of Pt film. In this way, in strong acidic solution, Pt deposition follows the Reactions 1 and 2, but in case of $\text{pH} > 2$, the intermediate ions of $[\text{Pt}(\text{OH})_m\text{Cl}_{6-m}]^{2-}$ contribute and follow the Reaction 4



Growth mechanism.—According to Pierce et al.,²¹ the first stage of electrodeposition involves the establishment of suitable boundary layer at the electrode surface, which thereafter starts to grow a thin film in second stage. The formation of initial boundary layer is very important stage for film growth, which is responsible for morphological change in the film. Therefore, it is needed to analyze the initial current density response for short time interval (10 s) that is shown in Fig. 1A. The current density show strong dependence on pH of electrolytic bath. Initially, current shows sudden rise and fall within short time interval that finally reaches to a plateau. The initial rise in current is due to accumulation of ions or formation of double layer charge on substrate surface,²² which is concerned with presence of electroactive nuclei in electrolytic bath. The double layer charging current decreases with pH , which reduces the electroactive nuclei and thus affects on film growth mechanism. This means electroactive nuclei decreases with pH of electrolytic bath. After double layer charge regime, current starts to reduce and reaches to plateau with steady state deposition behavior that concerns for continuous nucleation and growth of Pt film.

The plot of deposition current density (measured at 1000 s) vs pH of electrolytic bath is shown in Fig. 1B. It gives information about growth rate of Pt film on substrate surface. The deposition

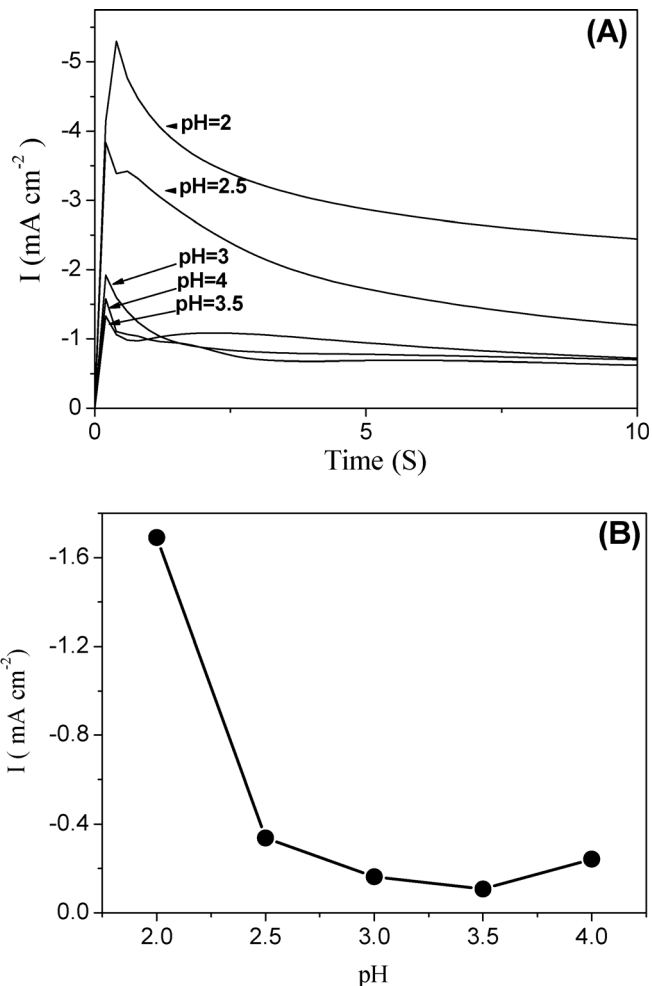


Figure 1. (A) The deposition current vs time (for initial 10) plot for Pt film deposited at different pH . (B) A plot of current measured at time 1000 S during the deposition process at different pH .

current density of Pt film deposited at pH 2 is high but it decreases up to pH 3.5 and show small rise in case of pH 4. The high current observed at pH 2 is concerning for combined contribution from hydrogen evolution on working electrode during film growth and Pt salt reduction. That current subsequently decreases with pH because of reduced hydrogen evolution. According to Hubbard et al.,²⁰ the reduction potential for $[\text{PtCl}_6]^{2-}$ takes place near to -0.25 V and it shifts to a higher potential (-0.30 V & onward) for intermediate ions of $[\text{Pt}(\text{OH})_m\text{Cl}_{6-m}]^{2-}$, which is depending on value of 'm'. The concentration of intermediate ion increases with pH that may increase the deposition current at pH 4.

In order to support this consideration, we have measured thickness of Pt film from depth profile plot of AES and values are given in Table I. The film thickness for a film deposited at pH 2 is ~ 30 nm and increases linearly up to 90 nm with pH . The film deposited at pH 2 shows high current (Fig. 1B) and low thickness (Table I), which reveals that hydrogen evolution also contributes to the deposition current. Above pH 2, the film thickness increases and deposition current decreases due to decreasing hydrogen evolution contribution.

The amount of Pt loading is calculated from the thickness by assuming bulk density of Pt as 21.45 g cm^{-3} and plotted with respect to pH . The roughness factor is calculated from the cyclic voltammeter plot by using hydrogen adsorption and desorption curve.²³ The amount of Pt loading was used for material loading and all the values of roughness factor and material loading are given in Table I. The amount of Pt loading shows strong dependence on

Table I. The thickness, roughness factor and amount of Pt loading values.

pH of electrolyte solution	Thickness (nm)	Roughness factor	Bulk density of Pt (g cm^{-3})	Amount of Pt loading ($\times 10^{-5} \text{g cm}^{-2}$)
2	30	2.68	21.45	2.44
2.5	63	2.19	21.45	6.16
3	68	2.18	21.45	6.68
3.5	75	1.09	21.45	14.75
4	90	0.62	21.45	—

pH of electrolytic bath. Low amount is observed ($2.44 \times 10^{-5} \text{g cm}^{-2}$) in a film deposited at pH 2 and the amount increases linearly up to $14.75 \times 10^{-5} \text{g cm}^{-2}$ with pH. The film deposited at pH 4 is not 100% covered {that's observed in SEM image (Fig. 2E)}; hence Pt loading for this film has not been calculated.

Surface morphological study.—The scanning electron microscopy (SEM) images of Pt film deposited at different pH are shown in Fig. 2. From figure it is seen that, all films show morphological changes from earth worm like structure to thorny ball with pH of electrolytic bath. Subramannia et al and Whalen et al have previously reported morphological changes in electrodeposited Pt film with respect to deposition potential.^{24,25} We also found the changes but with respect to pH of electrolytic bath. As seen from the figure, an earth worm like structure is observed in a film prepared at pH 2 (Fig. 2A), which is changed into dense and uniform surface morphology with pH (up to pH 3) (Fig. 2B) and (Fig. 2C), respectively. Highly agglomerated spherical grains with uniform structure are observed in a film prepared at pH 3.5 (Fig. 2D), which are subsequently changed into scattered thorny ball like structures with decreased surface coverage at pH 4 (Fig. 2E). The surface coverage is continuously decreased above pH > 4 and below pH < 2, hence these are not summarized in the present study.

XPS studies.—X-ray photoelectron spectrum (XPS) of Pt element in a film deposited at different pH of electrolytic bath is shown in Fig. 3. The films deposited up to pH 3 show only two peaks (a_1 & a_2), while at higher pH, it splits into three peaks of different intensity. All these peaks are related to Pt4f energy band, which after deconvolution show four peaks that correspond to the presence of pure Pt^0 (a_1 & a_2) and oxidized Pt (b_1 & b_2).²⁶ The peaks a_1 and b_1 reveals for the $\text{Pt}4f_{7/2}$ and its position gives information about presence of oxidized form of Pt. The pH of electrolytic bath varies the oxidation state of Pt film. Below pH 3, the film is in pure Pt^0 form but it undergoes oxidation with pH. The film deposited at pH 2 is

showing peak a_1 at binding energy around 71.6 eV, which is slightly decreased to 71.4 and 71.3 eV in a film deposited at pH 2.5 and 3, respectively. The observed small peak shift is negligible and corresponds to pure Pt^0 film. The binding energy shift becomes more prominent above pH 3, that observes at 71.7 (+0.5) eV and 72.1 (+0.9 eV) for pH 3.5, and pH 4, respectively. This binding energy shift may be prominent because of interaction with contaminated species inside the film material. The films deposited above pH 3 have a newly growing peak b_1 that corresponds to oxidized Pt, whose intensity is found to increase with pH. The intensity ratio of peak b_1/a_1 gives additional information about percentage of oxidized Pt in a film surface area. It turned out that about ~20% of film surface area exists in oxidized Pt form in the film deposited at pH 3.5, which subsequently increases to ~37% in the film deposited at pH 4. As we discussed above in growth mechanism, above pH 2 the $[\text{PtCl}_6]^{2-}$ ions (from electrolytic bath) undergo hydrolysis and form intermediate ions of $[\text{Pt}(\text{OH})_m\text{Cl}_{6-m}]^{2-}$ according to equation 3. Hence, above pH 3 the probable contribution of the intermediate ions of $[\text{Pt}(\text{OH})_m\text{Cl}_{6-m}]^{2-}$ increases that may entrap oxygen ions and the films become more oxidized at pH 3.5 and 4.

Evolution of active surface area by electrochemical process.—The catalytic activity of Pt film depends on available active surface area of the film for electrochemical reaction.²⁷ Hence, it needs to calculate the active surface area of Pt film that is calculated from cyclic voltammetry in N_2 purged H_2SO_4 solution. The active surface area of Pt film (dimension 1 cm^2) is measured by integrating hydrogen desorption curve of CV. During the reduction process on Pt film, proton from the acidic solution adsorbs on the surface of electrode while in case of oxidation, desorption takes place according to Reaction 5



After measuring the number of liberated electrons during oxidation, the number of hydrogen atoms desorbed from the Pt surface can be calculated. This defines the active surface of the film (A_r), which is used for calculation of specific catalyst area, $S(\text{m}^2 \text{g}^{-1})$ ²²

$$A_r = Q_{\text{H}}/Q_{\text{H}}^0 \quad [6]$$

$$S = (A_r)/(A_{\text{gW}}) \quad [7]$$

where,

Q_{H} —total charge associated with hydrogen desorption after double layer charge correction.

Q_{H}^0 —theoretical charge associated with plane Pt surface ($210 \mu\text{C}/\text{cm}^2$)

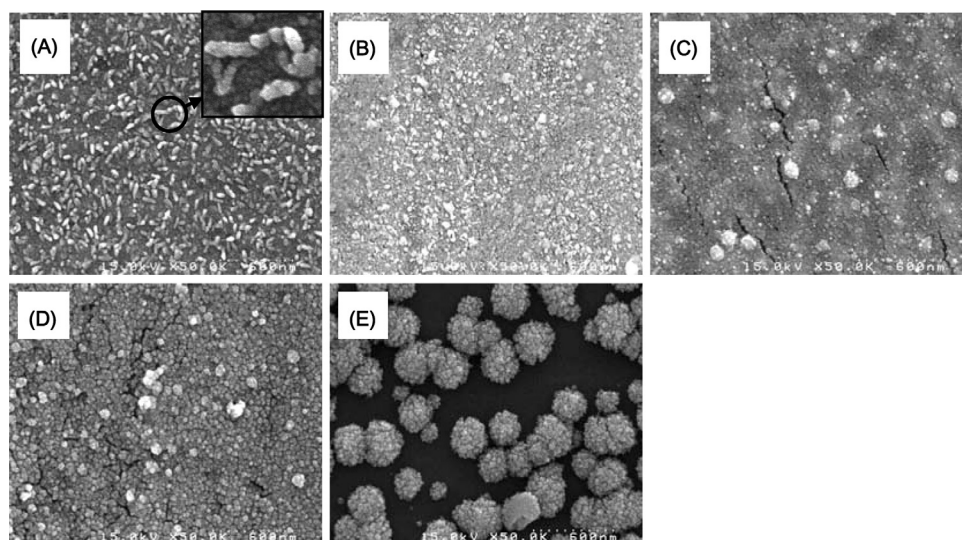


Figure 2. SEM images of Pt film deposited at different pH (A) pH 2 (B) pH 2.5 (C) pH 3 (D) pH 3.5 (E) pH 4.

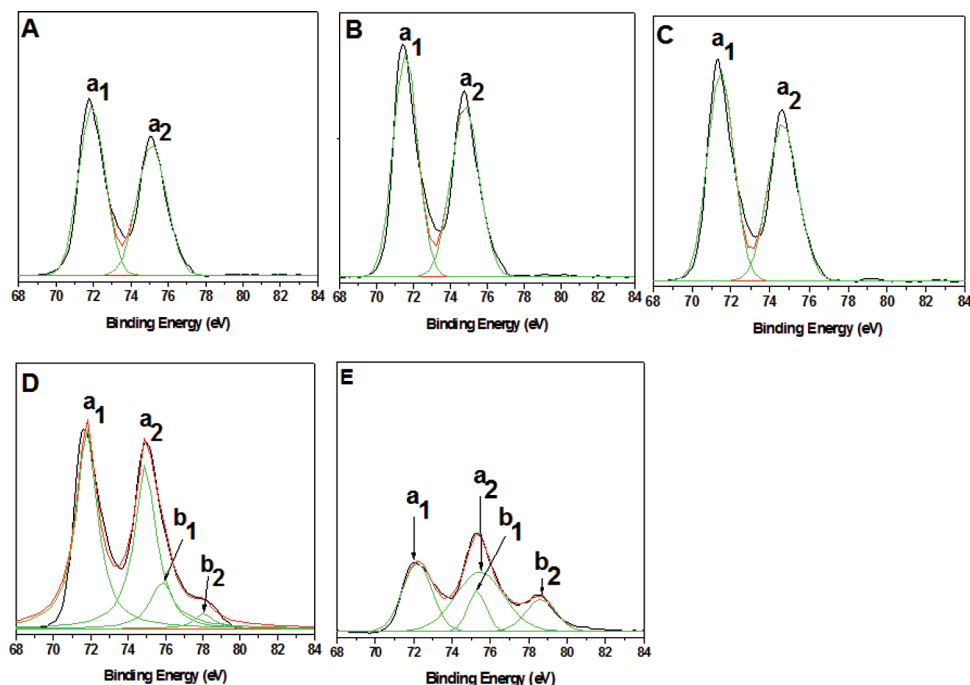


Figure 3. (Color online) XPS spectra of Pt film deposited at different pH (A) pH 2 (B) pH 2.5 (C) pH 3 (D) pH 3.5 (E) pH 4.

W–Pt loading (given in Table I)
Ag–geometric surface area (1 cm^2).

The specific catalyst area of Pt film is calculated from equation 7 and plotted with respect to pH, which is shown in Fig. 4. From figure it is seen that, the specific catalyst area of Pt film is decreased with pH. High active surface area ($98.5 \text{ m}^2 \text{ g}^{-1}$) is observed for a film deposited at pH 2 and subsequently decreases in a film deposited at pH 2.5 ($35.49 \text{ m}^2 \text{ g}^{-1}$) and pH 3 ($32.48 \text{ m}^2 \text{ g}^{-1}$). The surface morphology (from SEM Figs. 3A–3C) seems to be changed from rough surface (earth worm like structure) to highly uniform surface with pH. The surface area and surface roughness are relevant terms and directly proportional to each other. This is the reason for decreasing active surface area of Pt film with pH. The film deposited at pH 3.5 shows sudden drop down in active surface area ($7.412 \text{ m}^2 \text{ g}^{-1}$) due to surface passivation by oxide formation (XPS Fig. 4D). In case of pH 4, the surface area is very small ($2.294 \text{ m}^2 \text{ g}^{-1}$),

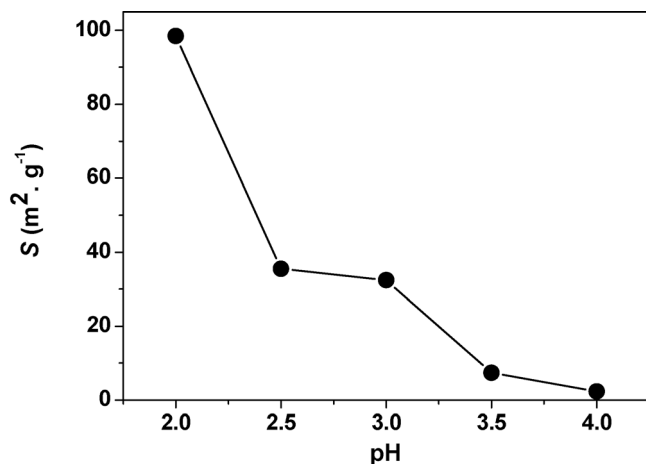


Figure 4. A plot of specific catalyst area (S) of Pt film deposited at different pH.

this is due to surface oxide formation and decrease in Pt surface area coverage.

Hydrogen production study.—The hydrogen evolution amount is measured 5 h with 1 h time lapse by using Pt film deposited at different pH as cathode electrode in photovoltaic (PV) cell assisted water electrolysis system. The average hydrogen evolution amount is plotted with pH of electrolytic bath, which is shown in Fig. 5. From figure it is seen that, the average hydrogen evolution amount decreases linearly with pH. It is observed about 525.6 ml h^{-1} in the film deposited at pH 2 that subsequently decreases to 515.2 ml h^{-1} (in the film deposited at pH 2.5), 511.8 ml h^{-1} (in the film deposited at pH 3) and down to 427.2 ml h^{-1} (in the film deposited at pH 4) with pH. According to Pournaghi–Azar et al, the catalytic activity of Pt film depends on available active surface area for electrochemical reaction, which increases with active surface area.²⁷ It means the

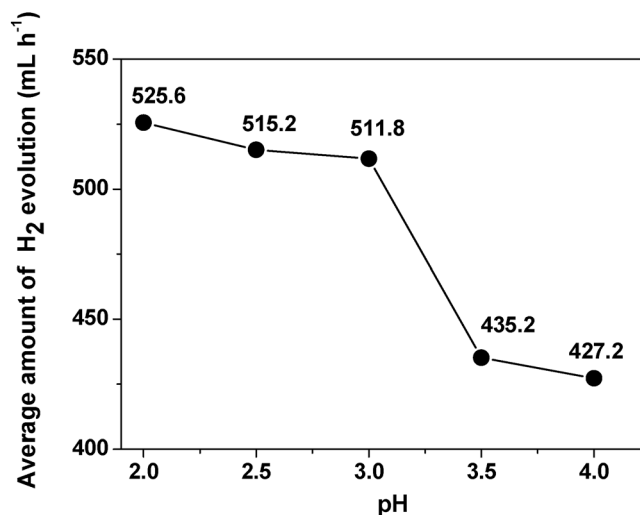


Figure 5. A plot of average amount of H₂ production (ml h^{-1}) for Pt film deposited at different pH.

active surface area is directly proportional to hydrogen evolution performance. Almost similar trend for both active surface area (Fig. 4) and hydrogen evolution performance (Fig. 5) is observed for Pt films deposited at different pH. According to Conway et al.,²⁸ Pt has more unpaired electron in d band, which interacts strongly with electron donating atoms or molecules such as hydrogen. Thus, hydrogen adsorbs strongly on Pt surface and forms electron pair with unpaired d electrons. The hydrogen evolution reaction is involving desorption of adsorbed hydrogen atom. It means rate of hydrogen evolution depends on rate of hydrogen desorption. In oxidized Pt film unpaired electrons form pairing with oxygen atom, which causes to reduce unpaired electrons for hydrogen adsorption and probably reducing the rate of hydrogen evolution. In case of film deposited at pH 3.5 and 4, the part of Pt is observed in oxidized form. This is another reason to decrease the hydrogen evolution performance. Thus, the Pt film deposited at pH 2 shows high hydrogen evolution performance and lower Pt loading than those of commercial Pt mesh.¹⁵ It is showing more than 25% higher hydrogen evolution and 1125 times less material loading than the commercial Pt mesh.

Conclusion

The growth of Pt film showed strong dependence on pH of electrolytic bath. At lower pH value, the Pt film growth was mainly contributed by $[\text{PtCl}_6]^{-2}$ ions and contribution of intermediate ions of $[\text{Pt}(\text{OH})_m\text{Cl}_{6-m}]^{2-}$ increased with pH. The pH of electrolyte bath also affected on the surface morphology, elemental composition and catalytic activity of the Pt film. It was observed as earth worm like structure in a film deposited at lower pH 2, which slowly changed into spherical grains with smooth surface up to pH 3.5 and subsequently changed into non-uniformly distributed thorny ball like structure in a film deposited at pH 4. The surface elemental compositional study showed that pure Pt film was obtained upto pH 3 and above this pH it undergo oxidation. The 20% surface area of the film prepared at pH 3.5 was in oxidized Pt form, which subsequently increased up to 37% in a film prepared at pH 4. The active surface area and hydrogen evolution performance showed almost linear relation and both proportionally decreased with pH. Thus, pure Pt film with minimum loading ($2.44 \times 10^{-5} \text{ g cm}^{-2}$), high active surface area ($98.5 \text{ m}^2 \text{ g}^{-1}$) and high hydrogen production (525.6 ml h^{-1}) was obtained in the film deposited at pH 2.

Acknowledgment

This work was funded by the “Hydrogen Energy R&D Center”, one of the 21st century frontier R&D programs, funded by Ministry of Science and Technology of Korea.

References

1. T. N. Veziroglu and F. Barbir, *Int. J. Hydrogen Energy*, **17**, 391 (1992).
2. I. P. Jain, *Int. J. Hydrogen Energy*, **34**, 7368 (2009).
3. H. Tributsch, *Int. J. Hydrogen Energy*, **33**, 5911 (2008).
4. Y. Cai, A. B. Anderson, J. C. Angus, and L. N. Kostadnov, *Solid-State. Lett.*, **8**, E62 (2005).
5. M. J. Cuetos, X. Gomez, A. Escapa, and A. Moran, *J. Power Sources*, **169**, 131 (2007).
6. R. K. Shervedani and A. Lasia, *J. Electrochem. Soc.*, **144**, 511 (1997).
7. M. P. Marceta Kaninski, D. L. Stojic, D. P. Saponjic, N. I. Potkonjak, and S. S. Miljanic, *J. Power Sources*, **157**, 758 (2006).
8. O. S. Joo, K. D. Jung, B. K. Min, S. H. Kim, and J. W. Oh, U.S. Pat. Application, 2008; 0131762A1.
9. M. J. De-giz, G. Tremiliosi-Filho, and E. R. Gonzalez, *Electrochim. Acta.*, **39**, 1775 (1994).
10. D. L. Stojic, B. D. Cekic, A. D. Maksic, M. P. Marceta Kaninski, and S. S. Miljanic, *Int. J. Hydrogen Energy*, **30**, 21 (2005).
11. S. Licht, B. Wang, S. Mukerji, T. Soga, M. Umeno, and H. Tributsch, *J. Phys. Chem. B*, **104**, 8920 (2000).
12. B. Yazici, *Turk. J. Chem.*, **23**, 301 (1999).
13. R. M. Q. Mello and E. A. Ticianelli, *Electrochim. Acta.*, **42**, 1031 (1997).
14. L. F. Petrik, Z. G. Godongwana, and E. I. Iwuoha, *J. Power Sources*, **185**, 838 (2008).
15. J. B. Yadav, J. W. Park, K. D. Jung, and O. S. Joo, *Int. J. Hydrogen Energy*, **35**, 6541 (2010).
16. C. R. K. Rao and D. C. Trivedi, *Coord. Chem. Rev.*, **249**, 613 (2005).
17. M. E. Baumgartner and C. J. Raub, *Platinum Met. Rev.*, **32**, 188 (1988).
18. J. Iniesta, J. Gonzalez-Garcia, J. Fernandez, V. Montiel, and A. Aldaz, *J. Mater. Chem.*, **9**, 3141 (1999).
19. L. Y. Lau and T. Hubbard, *J. Electroanal. Chem.*, **24**, 237 (1970).
20. A. T. Hubbard and F. C. Anson, *Anal. Chem.*, **38**, 1887 (1966).
21. P. E. Pierce, Z. Kovac, and C. Higginbotham, *Ind. Eng. Chem. Prod. Res. Div.*, **17**, 317 (1978).
22. F. Gloaguen, J. M. Leger, C. Lamy, A. Marmann, U. Stimming, and R. Vogel, *Electrochim. Acta.*, **44**, 1805 (1999).
23. A. S. A. Khan, R. Ahmed, and M. Latif Mirza, *Portugaliae. Electrochim. Acta.*, **27**, 429 (2009).
24. M. Subhramannia, K. Ramaiyan, and V. K. Pillai, *Langmuir*, **24**, 3576 (2008).
25. J. J. Whalen III, J. D. Weiland, and P. C. Seanson, *J. Electrochem. Soc.*, **152**, C738 (2005).
26. J. F. Moulder, W. F. Stickle, P. E. Sobol, and K. D. Bomben, *Handbook of X-ray Photoelectron Spectroscopy*, 1st ed., J. Chastain, and R. C. King, Editors, pp. 180–181, Physical Electronics Inc, US (1995).
27. M. H. Pourmaghi-Azar and A. B. Habibi, *J. Electroanal. Chem.*, **580**, 23 (2008).
28. B. E. Conway and J. O. Bockris, *J. Chem. Phys.*, **26**, 532 (1957).